流下液膜に生ずる馬蹄形表面波（渦）の運動特性

Shadowgraphic observation of surface waves on a water film falling inside a vertical tube and the associated gas absorption

C.D. Park[a], T. Nosoko[a], A. Miyara[b], T. Nagata[a] and S.T. Ro[c]

[a]*Department of Mechanical and Systems Engineering, University of the Ryukyus, Nishihara, Okinawa 903-0213, Japan*

[b]*Department of Mechanical Engineering and Systems, Saga University, Saga 840-8502, Japan*

[c]*Department of Mechanical Engineering, Seoul National University, San 56-1, Shilim-dong, Kwanak-gu, Seoul, 151-742, Korea*

Abstract

The dynamics and the associated gas absorption rates of naturally evolving and periodically triggered surface waves on water film falling inside a vertical tube have experimentally been investigated. It was found that the transition from laminar to turbulent flow occurs within Reynolds number range of $400 \lesssim Re \lesssim 700$, along with a drastic increase in the Sherwood number *Sh*. Furthermore, a new transition was found to occur at $Re \approx 40$ in the laminar flow region, where the dynamics of waves significantly changes and a sudden decrease in the power n of the correlation $Sh = CRe^n$ is observed. Imposing the periodic disturbances on film flow shortens the transition range of *Re*, causing the turbulent flow inception to occur much more upstream and the associated gas absorption to enhance especially in shorter tube.

1. Introduction

Liquid films falling down a surface are widely encountered in nature as well as in industrial process equipment such as steam condensers, wetted wall absorbers and liquid film evaporators. It is well known that surface waves on falling film enhance the gas absorption into the film in the laminar flow region (Seban and Faghri, 1978). At low Reynolds numbers in the laminar region, each surface wave consists of a large-peak roll wave with a continuous wavefront and front-running capillary waves having small amplitudes. Nagasaki and Hijikata (1989) and Miyara (2000) performed numerical simulations and analysis, respectively, and found that each roll wave holds a flow circulation whose size and strength increase with the roll wave size. By experimentally determining the dynamics of the roll waves on films falling down a vertical surface and the associated gas absorption at $Re < 80$, Nosoko et al. (1996) and Yoshimura et al. (1996) showed that the flow circulations in the roll waves play an important role in the gas absorption enhancement. Bakopoulos (1980) constructed empirical correlations of the Sherwood number Sh for long films falling down a vertical surface based on experimental data by Kamei and Oishi (1956) and other researchers, indicating that the transition to turbulent film flow occurs at $Re = 400$ and that a sudden decrease in the power n of the correlation $Sh = CRe^n$ occurs at $Re = 70$. Hikita, et al. (1959) and Nakoryakov, et al. (1983) likewise pointed to the existence of the decrease in the power n at $Re = 40 - 75$, based on experimental measurements of the gas absorption into films or desorption from films. These sudden decreases in the power n imply that a transition of flow occurs at such Re's. Unfortunately, due to the complex behavior of surface waves, what occurs in the film flow and in the dynamics of surface waves at these Re's is still unclear and has not been fully investigated.

In the present work, periodic disturbances were imposed on the film flow at the film inlet to produce surface waves of relatively regular behavior. These waves were observed by shadowgraphy and their gas absorption rates were determined at various Reynolds numbers. The transition to the turbulent flow and a new transition in the laminar flow region are also discussed based on the observations of wave dynamics and the gas absorption.

2. Experimental apparatus and procedure

The experimental apparatus for gas absorption and shadowgraphic optical arrangement are schematically shown in Fig. 1. Tap water, cooled by flowing through a coiled copper tube submerged in a temperature-controlled water bath (not shown in Fig. 1), is led to the head tank. As shown in Fig. 1 (a), the water flows from the head tank to the top of a 9.6 mm inner diameter vertical glass tube where it is evenly distributed through 17 capillary tubes of 1.5 mm inner diameter to form a water film on the inner surface of the glass tube. Concurrently, oxygen gas from a gas cylinder is made to flow into the glass tube from its base after passing through a bubbling water bottle. The resulting oxygen rich water from the glass tube is passed through a bubble separator into a measuring cell where the water is stirred, and the dissolved concentration of oxygen C_{out} and the temperature are measured with a dissolved oxygen meter probe equipped with an ammeter (model OE-2101 and DO-25A, produced by Toa-Denpa Co. Japan). To measure the dissolved oxygen concentration C_{in} at the film inlet, tap water was directly introduced into the measuring cell prior to and immediately after each series of experimental runs. The volumetric water flow rate out of the cell was likewise measured.

The water temperatures were measured by the calibrated T-type thermocouples at

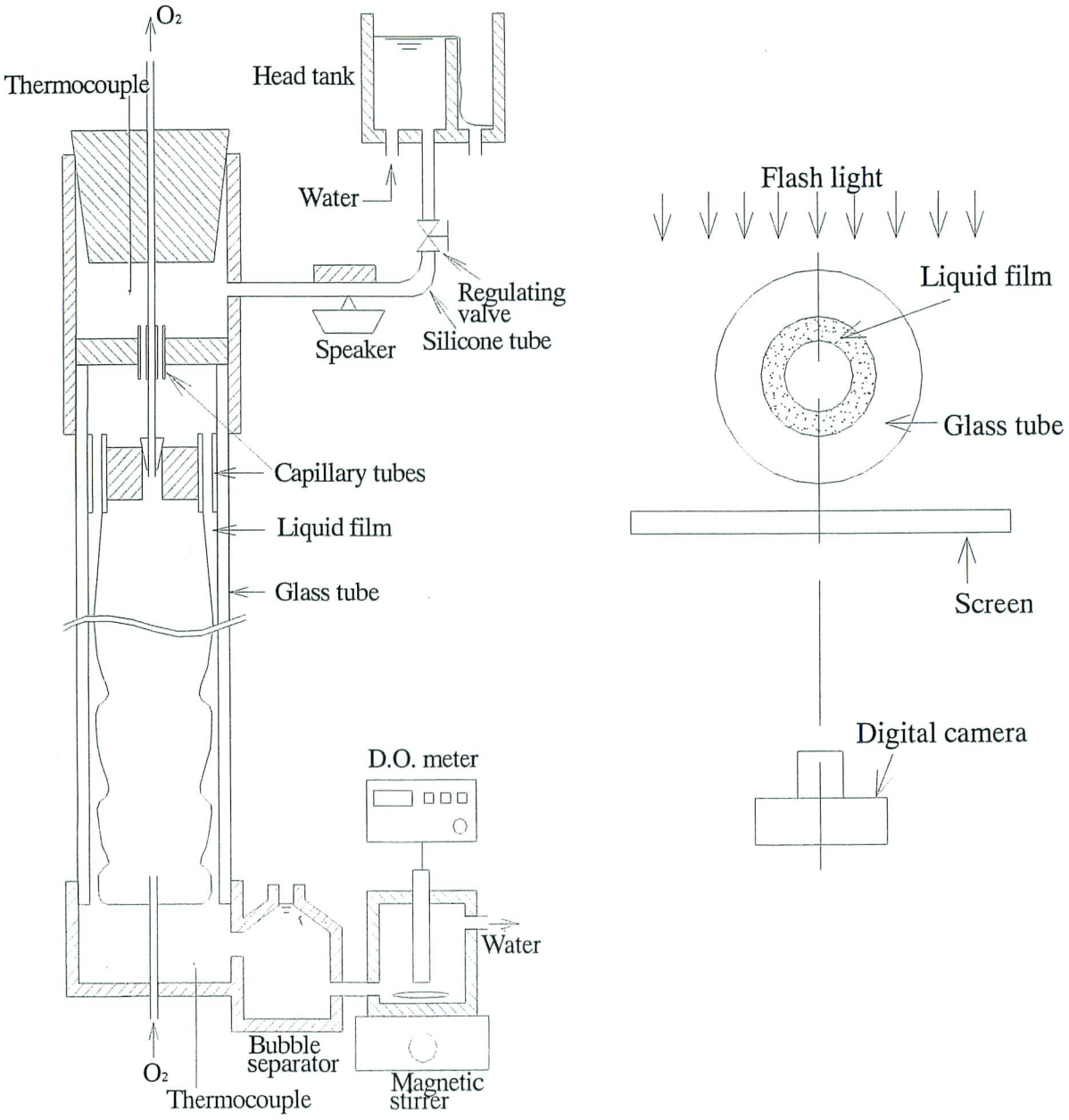

(a) Flow diagram (b) Optical arrangement

Fig. 1 Experimental apparatus

the inlet and exit of the film. The film temperature T_f was assumed as the mean value of these inlet and outlet temperatures of the flow. The experiments were performed at a film temperature range of 10 - 24 °C. A thin plastic plate fixed to the vibrating cone of a speaker vibrates the silicone tube with its edge to impose the periodic disturbances on the water flow in the tube as well as the film at its inlet.

Figure 1 (b) shows the shadowgraphic optical arrangement with flashing light from a stroboscope passing through the water film in the glass tube and forming shadow of wave on the screen. This shadow was captured by a camera synchronized with the stroboscope.

3. Equations for the mean mass transfer coefficient and dimensionless groups

The Reynolds number Re and the Sherwood number Sh, formulated in terms of the mean film thickness δ, are defined as $Re = \Gamma/\nu$ and $Sh = k\delta/D$, respectively, where Γ is the volumetric flow rate of water per unit length of wetted perimeter, ν is the kinematic viscosity of liquid, D is mass diffusivity and k is the mass transfer coefficient. The values D can be derived from the Stokes-Einstein equation (Bird et al, 1960).

The mean film thickness δ for laminar and turbulent flow can be calculated using the correlation of the Nusselt film thickness and the empirical correlation by Brauer (1956), respectively:

for laminar flow: $$\delta = \left(\frac{3\nu^2 Re}{g}\right)^{1/3} \qquad (1)$$

for turbulent flow: $$\delta = 0.302\left(\frac{3\nu^2}{g}\right)^{1/3} Re^{8/15} \qquad (2)$$

where g is the acceleration of gravity.

Assuming constant mass transfer coefficient, the mean mass transfer coefficient k is given as:

$$k = \frac{\Gamma}{\pi(d-2\delta)L_t} \ln \frac{C_S - C_{in}}{C_S - C_{out}} \qquad (3)$$

where L_t is the film length and $\pi(d-2\delta)L_t$ is the area of the film surface.

4. Results and Discussion

4.1 Dynamics of surface waves

Figure 2 shows the shadows of the surface waves in the Reynolds number range Re = 20 - 800 on the water film over a distance of $x \leq 0.4$ m below the film inlet. When periodic disturbances are not imposed on the film flow, surface waves quickly become visible at a distance from the film inlet, and then travel downstream. A smooth surface appears just below the film inlet, and the length L_{sm} of this surface increases with Re up to a maximum at $Re \approx 400$ after which it rapidly decreases and disappears (see Fig. 3). These values obtained are in fairly good agreement with the results by Tailby & Portalski (1962) at $20 \lesssim Re \lesssim 400$.

When the periodic disturbances were imposed on the film flow, waves occur just below the film inlet causing the smooth surface to disappear at $Re \lesssim 400$ (see Fig. 2 (b)). The film flow inertia increases with Re, while the power of disturbances relative to the flow inertia decreases. Although nearly smooth surfaces are observed below the film inlet at $400 \lesssim Re \lesssim 600$, their lengths are much shorter than those observed when no periodic disturbances were imposed.

The behavior of the 'forced' waves evolving from the periodic disturbances is basically the same as that of the naturally occurring waves after their inception. The

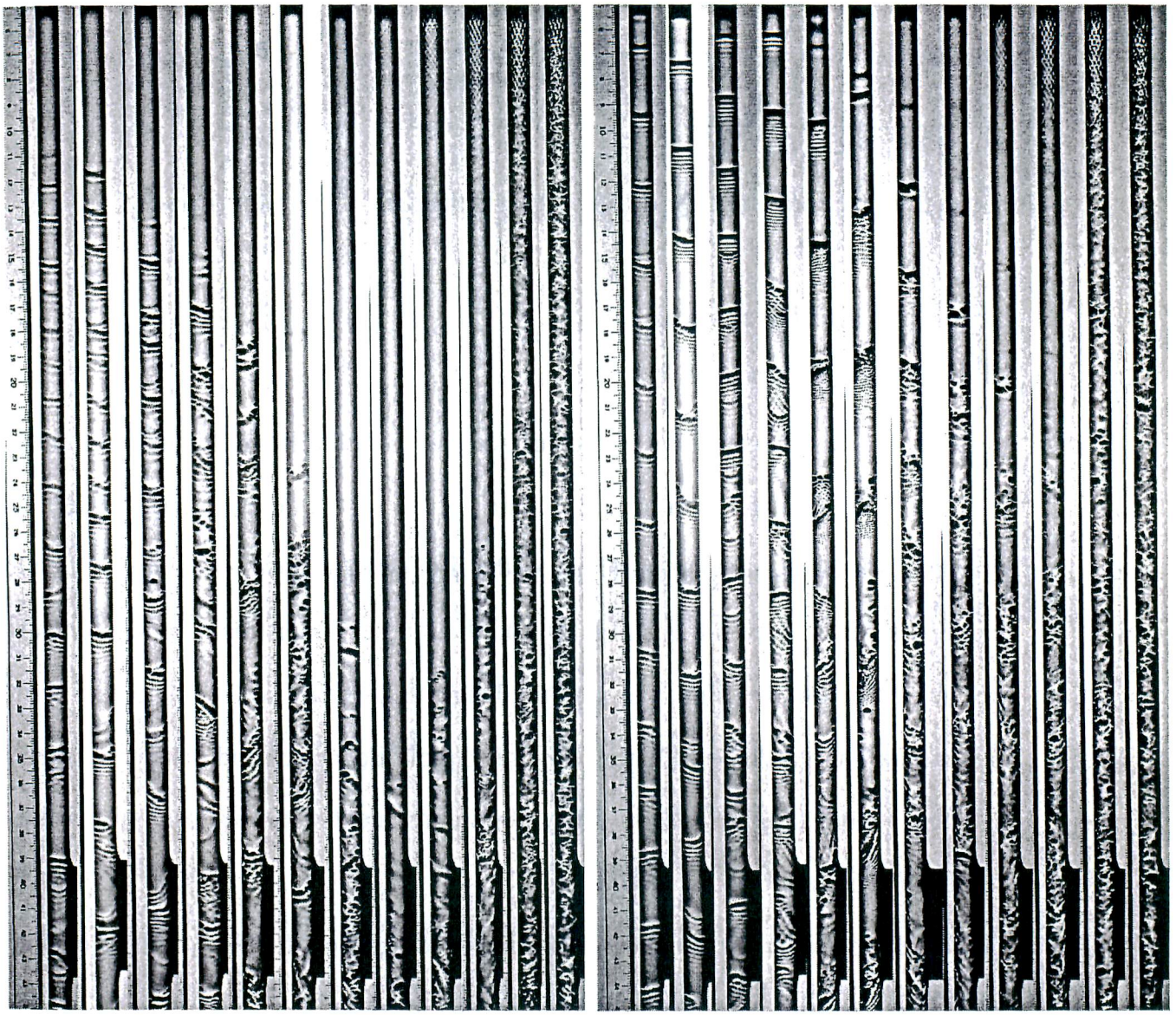

Re	20.4	32.2	40.2	64.2	129	200	302	399	503	603	707	806
f	0											

Re	20.4	32.2	40.2	64.2	129	200	302	399	503	603	707	806
f	12 Hz		15 Hz				30 Hz					

(a) Without the periodic disturbances (b) with the periodic disturbances

Fig. 2 Photographs of surface wave shadows

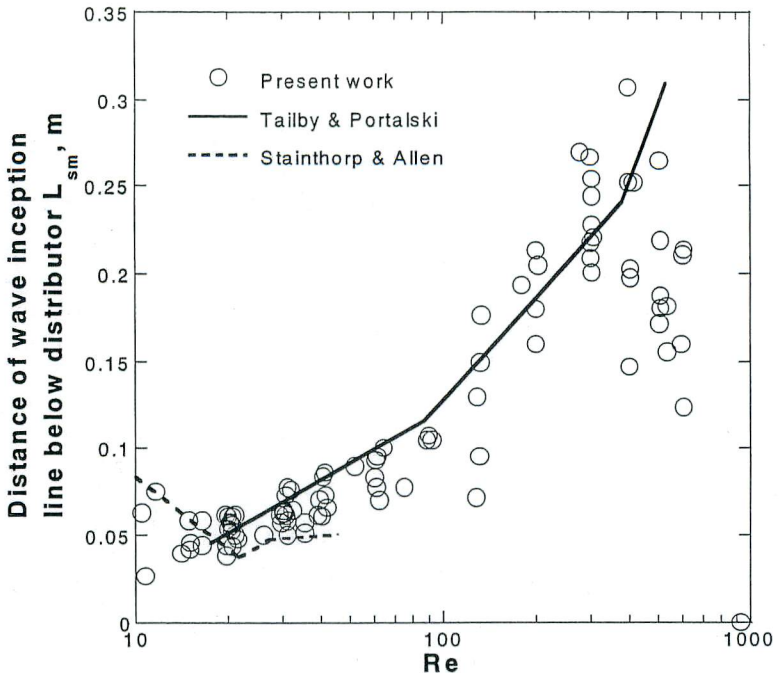

Fig. 3 Variation of smooth film lengths L_{sm} with Re

Fig. 4 Development of the surface wave

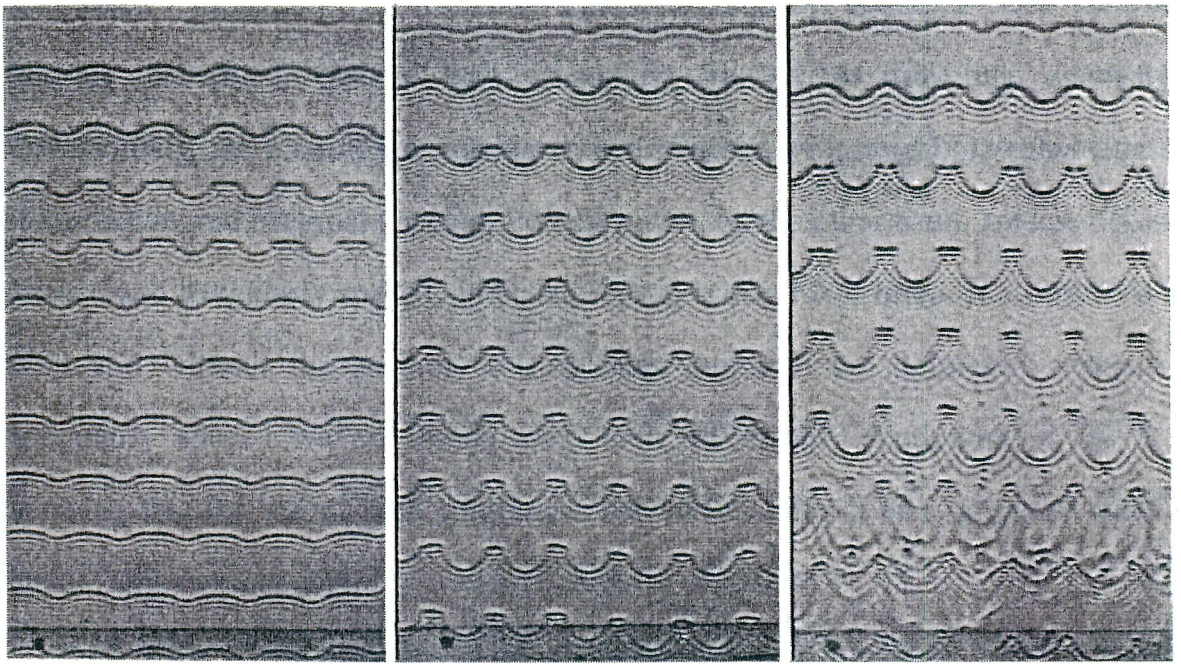

(a) Re = 30 (b) Re = 41 (c) Re = 65

Fig. 6 Evolution of transverse deformation of waves

behavior of waves can be more clearly described by the forced waves in Fig. 2. At $Re \lesssim 40$, waves with almost horizontal and continuous wavefronts appear (seen as the dark lines with high contrast in photographs of Fig. 2), and then these wavefronts become deformed, slanted and irregularly spaced as traveling downstream. Occasionally, the naturally occurring waves coalesce with neighbors enhancing their deformation and irregular spacing. Forced waves, on the other hand, are less deformed, slanted and irregularly spaced, and coalitions also occur less often. It is observed that, with and without the periodic disturbances imposed, the deformed, slanted and irregularly spaced waves always keep their wavefronts continuous at $Re \lesssim 40$, showing that the waves with continuous wavefronts consist of a large roll wave and small front-running capillary waves (Nosoko et al., 1996).

At $40 \lesssim Re \lesssim 400$, wavefronts are continuous at their inception, but they gradually disintegrate into fragments and dimples (seen as dark spots) as they travel downstream, resulting in appearance of rough surfaces with the fragments and dimples separated by nearly smooth (or much less rough) surfaces. The rough surfaces gradually expand over the nearly smooth surfaces as the waves travel downstream. This wave disintegration is clearly displayed in Fig. 4. Horizontal wavefront deforms to sharp bends, where the wavefront begins to disintegrate into a number of dimples.

At $Re \gtrsim 400$, waves with continuous wavefronts are not observed even at inception, but a few dimples appear at first with new ones continuously appearing as the film travels downstream. The first dimples appear at a shorter distance x as the Re increases. The imposed periodic disturbances cause dimples to appear at much shorter distance from the film inlet, shortening the nearly smooth surface below the inlet at $400 \lesssim Re \lesssim 700$. (It is seen a mesh-like shadow just below the film inlet in the

photographs at $400 \lesssim Re \lesssim 700$, which represents an interaction among jets from the capillary tubes.) At $Re \gtrsim 700$, dimples appear just below the film inlet, and the whole film surface is covered with dimples. The number of dimples or the roughness of film surface, i.e. the amplitude of dimples increases with Re especially in $0 < x \lesssim 0.3$ m at $400 \lesssim Re \lesssim 700$. The imposed periodic disturbances do not cause noticeable change in the film surface structure at $Re \gtrsim 700$.

4.2 Mass transfer

Variations of Sherwood number Sh with Reynolds number Re at film height L_t = 0.37 m and 0.95 m are shown in Fig. 5, which are compared with empirical correlations constructed based on experimental data for naturally occurring waves by Bakopoulos (1980) and by Hikita et al (1959). The solid lines fit the present data obtained with the periodic disturbances imposed on the film. The correlations by Hikita et al. fit their own experimental data for 0.2 - 1.03 m high films of water, butanol, methanol aqueous solution and sugar aqueous solution, which were produced by an overflowing distributor. Those by Bakopoulos are constructed based on experimental data by Kamei and Oishi (1956) and other researchers for 0.6 - 2.5 m high water films produced by overflowing and uniform gap channel distributors.

Comparison between forced waves and naturally occurring waves

For the short water film (0.37 m high), the naturally occurring waves have a slightly smaller Sh than forced waves at $Re \lesssim 80$. The difference in Sh increases with Re by much as 73 % at $Re \approx 400$ and then rapidly decreases within $400 \lesssim Re \lesssim 700$ to be zero at $Re \gtrsim 700$. This variation of the discrepancy in Sh corresponds to that of the smooth surface length L_{sm} shown in Fig. 3. The length L_{sm} rapidly increases with Re at

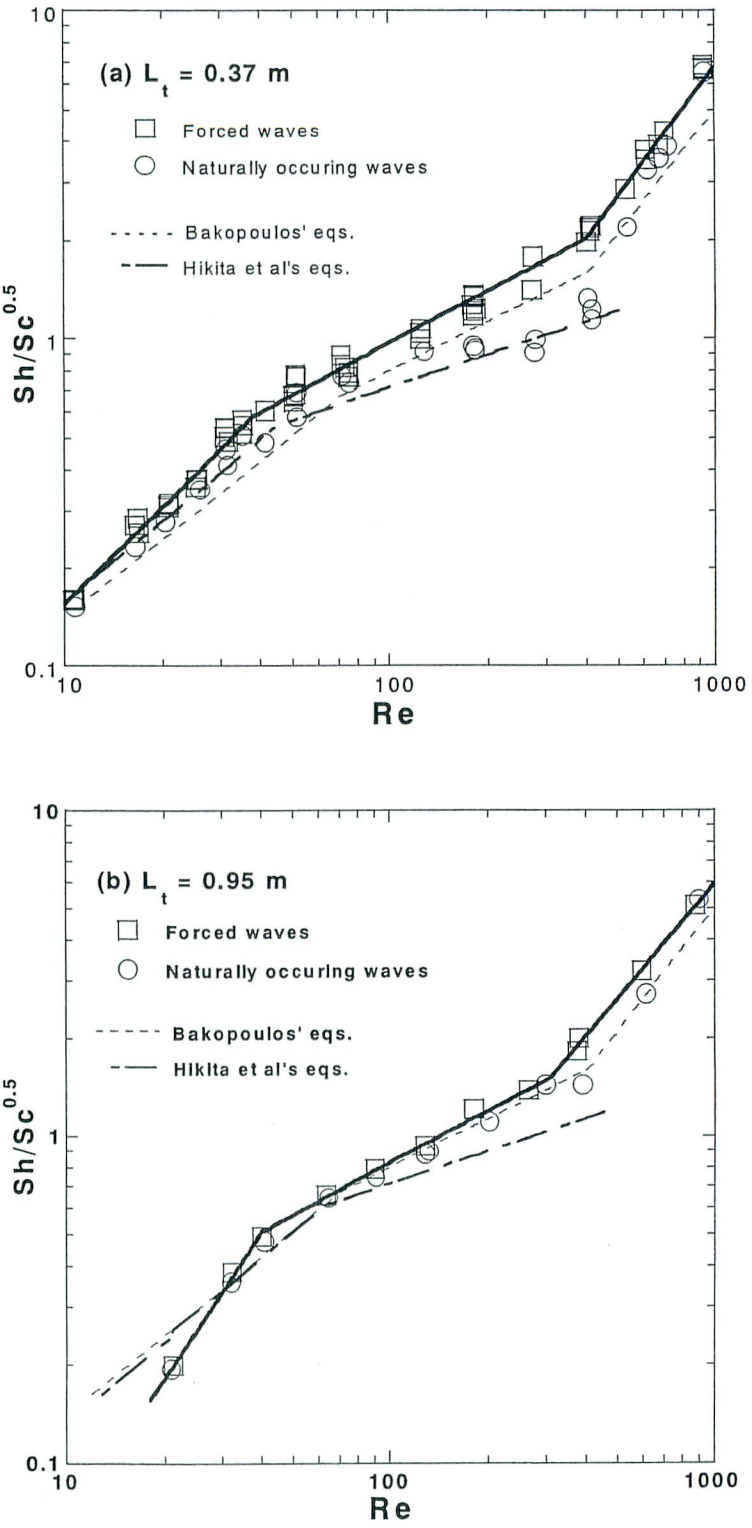

Fig. 5 Variation of Sh with Re

$Re \gtrsim 70$ up to the maximum at $Re \approx 400$, and then drastically decreases to zero, indicating that surface waves greatly increase the mass transfer. Nosoko, et al. (1996) experimentally showed that surface waves hold a flow circulation in each roll wave and enhance the mass transfer up to 2.3 times the transfer rate for a smooth film surface. The circulation causes a mixing of the boundary layer developing along the film surface in front of the roll wave and renews the surface just behind the roll wave to carry fresh liquid from the bulk to the surface.

In the case of the long water film (L_t = 0.95 m), there is either no or only slight difference in *Sh* between forced waves and naturally occurring waves. The reasons are that the ratio of L_{sm} is much smaller in comparison with the surface length (L_t - L_{sm}) covered with waves and such decrease in *Sh* due to the short smooth surface is insignificant. The maximum of the ratio L_{sm}/L_t is only about 0.24 at $Re \approx 400$.

The correlations by Hikita et al. as functions of film length L_t, are only applicable to short films at $Re \lesssim 400$. Though these correlations agree well with the present results for the naturally occurring waves on the 0.37 m long film, they fail to predict *Sh* for the 0.95 m long film. The correlations by Bakopoulos, which do not depend on the film length, are applicable to long films of $L_t \gtrsim 1$ m. The correlations correspond well with the present data for the 0.95 m long film in the entire *Re* range except at $Re \lesssim 40$ where the present values of *Sh* agree fairly with the correlation but there is a large difference in the slope of line in Fig. 5 (b), i.e. the increasing rate of log *Sh* with log *Re*. This can be attributed to the widely scattered experimental data on which the Bakopoulos' correlation is based, and to poor experimental accuracy of mass transfer coefficient *k* at low *Re* for long films where values of (C_S - C_{out}) in eq. (3) become very small, thus raising the error of *k*.

Transition to turbulent film flow

The drastic increase of Sh at $400 \lesssim Re \lesssim 700$ in Fig. 5 (a) and the sharp decrease of L_{sm} in Fig. 3 indicate that the transition from laminar to turbulent flow occurs at $400 \lesssim Re \lesssim 700$ in the film without the periodically imposed disturbances. Takahama and Kato (1980) determined this transition to turbulent flow by measuring the variation of time-average film thickness δ with Re experimentally, and found that the transition occurs far downstream at the critical Reynolds number $Re_{ct} \approx 400$ and Re_{ct} rapidly increases from 400 up to 800 with decreasing distance x from the film inlet. Their findings correspond with the present observations, i.e. the sharp decrease of L_{sm} to zero and the drastic increase of Sh with Re at $400 \lesssim Re \lesssim 700$.

Slight discrepancies between previous results and those we obtained, e.g. the increase in Re_{ct} from 400 to 800 with a decrease in x from 1.3 m to 0.8 m and the one from 400 to 700 with x from 0.3 - 0.2 m to zero, were observed. These may be attributed to the fact that Takahama and Kato employed an overflowing distributor to produce water films whereas the water films used in present experiment were produced from capillary tubes arranged in a ring shape. Since film flow from the overflowing distributor includes noise of much smaller amplitude, it takes a longer distance x and larger flow rate to change into turbulent flow. In addition, the film surface observed by shadowgraphy and the variation of Sh with Re are much more sensitive to turbulent flow and, as such, may detect the inception of turbulent flow, whereas the variation of average film thickness detects the fully developed turbulent flow.

The forced waves may cause the transition to turbulent flow to occur at much

shorter distances, and therefore prevent a marked increase in Sh at $Re \approx 400$ (Fig. 5). When the periodic disturbances are not imposed on the 0.95 m long film, the transition to turbulent flow occurs at distances x which have small ratios to the total film length, and therefore slight difference in Sh from the forced waves is observed at $400 \lesssim Re \lesssim 700$ in Fig. 5 (b).

Transition of dynamics of waves in laminar flow region

The variations of Sh with Re obtained in the present work and the correlations by Bakopoulos and Hikita et al. all indicate the existence of some transition of film flow at Re = 40 - 70 where the slope of the log Sh - log Re line suddenly varies (Fig. 5). The correlations by Hikita et al. show that the critical Reynolds number Re_{cw} at this transition increases from 40 to 60 with an increase in the film length L_t from 0.2 m to 1.0 m since the effects of the smooth surface length on Sh are significant for short films. The correlations by Bakopoulos have the fixed Re_{cw} = 70 for the transition. Because of widely scattering experimental data from which such correlations were constructed, his value for Re_{cw} may be inaccurate. The present data obtained with the 0.95 m long film show that the transition occurs at $Re_{cw} \approx 40$ whether the periodic disturbances are imposed or not. Results obtained for the 0.37 m long film covered with forced waves also show the same value for Re_{cw}.

To observe the waves more clearly, transverse disturbances were imposed on periodically forced waves on a water film flowing down a vertical plane by putting tips of needles into the film just below a uniform clearance distributor at constant intervals of 20 mm, and the forced waves were observed by shadowgraphy (refer Nosoko, et al. (1996) for details of experimental setup). Figure 6 shows shadows of

waves at different Re with evolving transverse deformation of wavefronts. At $Re \lesssim 40$, the amplitudes of the forced waves increase from the transverse deformation at first and then decrease as the waves travel downstream (Fig. 6 (a)). At $Re \approx 40$, the waves show a saturation of an increase in the amplitude, and then travel downstream with little change in wave shape and speed (Fig. 6 (b)). Figure 6 shows more clearly that at $Re \lesssim 40$ the waves always keep continuous wavefronts, i.e. the wavefronts of the roll wave with front-running small capillary waves. At $Re \gtrsim 40$, the amplitude of the waves monotonously increase to become U-shaped with sharp bends between the 'U's where the wavefronts disintegrate into dimples. The 'U's interact with the front-going waves to disintegrate into fragments. Even when such transverse disturbances are not imposed on the film flow, the wave disintegration into fragments and dimples occurs more slowly as shown in Figs. 2 and 4.

The flow inside the dimples and bumps among dimples may behave differently from the flow inside the roll waves having continuous wavefronts. Therefore the characteristics of the associated mass transfer are different between at $Re \lesssim 40$ and $40 \lesssim Re \lesssim 400$ as exemplified in Fig. 5.

5. Conclusions

The present shadowgraphic observations of surface waves on falling water films and the experimental measurements of the associated gas absorption rates of the films may be summarized as follows:

1. A transition in wave dynamics occurs in laminar film flow region at $Re \approx 40$ at which the slope of the log Sh - log Re line suddenly decrease. At $Re \lesssim 40$, the waves always keep their wavefronts continuous with a distinct roll wave-capillary structure, but they disintegrate into fragments and dimples at $Re \gtrsim 40$.

2. The transition from laminar to turbulent flow occurs in falling films at $400 \lesssim Re \lesssim 700$ where there is a drastic increase in Sh and where turbulent flow inception moves upstream with Re. The imposition of the periodic disturbances on film flow shortens the transition range of Re, causing the turbulent flow inception to occur much more upstream.

Acknowledgement - The authors gratefully acknowledge Mr. S. Oyakawa and Mr. T. Shimada for their assistance in this experiment. This work was supported by TEPCO Research Foundation and Japan Society for the Promotion of Science (Project No. 11650231).

Reference

A. Bakopoulos, Ger. Chem. Eng., Vol. 3, pp. 241-252, 1980.

A. Miyara, International Journal of Thermal Sciences, Vol.39, pp.1015-1027, 2000.

B.R. Seban and A. Faghri, J. Heat Transfer, 100, 143-147, 1978.

F.P. Stainthorp and J.M. Allen, Trans. Instn Chem. Engrs., Vol. 43, T85-T91, 1965.

R.B. Bird, W.E. Stewart and E.N. Lightfoot, Transport Phenomena, Wiley, New York, 1960.

H. Brauer, Stromung and Warmeubergang bei Rieselfilmen, VDI (Ver. Deut. Ingr.) – Forschungshelt, 457, 1956.

H. Hikita, K. Nakanishi, and T. Kataoka, Chem. Eng. (Japan), Vol. 23, No.7, pp. 459-466, 1959.

H. Takahama and S. Kato, Int. J. Multiphase Flow, Vol. 6. pp. 203-215, 1980.

P.N. Yoshimura, T. Nosoko and T. Nagata, Chem. Eng. Sci., Vol. 51, pp. 1231-1240, 1996.

S. Kamei and J. Oishi, Mem. Fac. Eng., Kyoto Univ. **18** 1, 1956

S.R. Tailby and S. Portalski, Chem. Eng. Sci., Vol. 17, 283-290, 1962.

T. Nagasaki, and K. Hijikata, In ANS Proceedings 1989 National Heat Transfer Conference, Vol. 4, pp. 23-30, 1989.

T. Nosoko, P.N. Yoshimura, T. Nagata and K. Oyakawa, Chem. Eng. Sci., Vol. 51, No. 5, pp. 725-732, 1996.

V.E. Nakoryakov, G.G. Pokusaev and S.V. Alekseenko, Theoretical foundation of Chem. Eng., Vol. 17, pp. 199-204, 1983.